



Innovative performance-based design of slope stabilizing piles for a railway embankment

Andrea Galli & Andrea Bassani

To cite this article: Andrea Galli & Andrea Bassani (2016): Innovative performance-based design of slope stabilizing piles for a railway embankment, European Journal of Environmental and Civil Engineering, DOI: [10.1080/19648189.2016.1179681](https://doi.org/10.1080/19648189.2016.1179681)

To link to this article: <http://dx.doi.org/10.1080/19648189.2016.1179681>



Published online: 29 Apr 2016.



Submit your article to this journal [↗](#)



Article views: 73




View related articles [↗](#)



View Crossmark data [↗](#)

Innovative performance-based design of slope stabilizing piles for a railway embankment

Andrea Galli^{a*}  and Andrea Bassani^b

^aDipartimento di Ingegneria Civile e Ambientale, Politecnico di Milano, Milano, Italy; ^bDesign of Sustainable Construction, Erba, Italy

(Received 6 November 2015; accepted 12 April 2016)

The paper presents a simplified displacement-based approach for the design of a slope stabilising system. On the top of the slope, a railway ballasted track induces repeated dynamic loads on the subgrade soil, that, in conjunction with other cyclic environmental loads (seasonal temperature and soil moisture variation) induce a progressive accumulation of soil displacements, despite the safety factors for the slope, if computed by means of traditional limit equilibrium methods, are all larger than one. The design procedure started then from the analysis of preliminary (pre-operam) monitoring data, in order to define the shape and amplitude of the soil displacement field, by interpreting them within a viscoplastic constitutive framework. This allowed to conveniently optimise the slope stabilising system (consisting in FRC piles connected to each other by means of a precast FRC beam and reinforced by pre-stressed ground anchors) with the aim of reducing the soil displacement rates below a prescribed threshold. The focus of the work, rather than presenting advanced constitutive or numerical simulations, is on the design approach, which allows the designer to get a reliable and safe design solution, even in lack of rich and sophisticated site characterisation, as it is often the case in real applications.

Keywords: slope stabilising piles; displacement-based design; viscoplastic approach; on site monitoring; soil-structure interaction

1. Introduction

The design of slope stabilising structures is a complex problem requiring the engineer to carefully take into account several factors, such as: (i) the geometry of the slope, (ii) the mechanical properties of the materials constituting the slope, (iii) the type and intensity of favourable and unfavourable actions, (iv) the shape and the amplitude of the unstable soil displacement profile. This latter issue requires of course an accurate (and sometime apparently expensive) preliminary monitoring phase of the slope, but it is one of the most important points to be addressed when actual risk mitigation measures have to be implemented (i.e. before the triggering of a landslide), and it represents even the only possible way to assess the long-term effectiveness of the intervention. Moreover, the shape and the amplitude of the soil displacement profile largely affect the stress distribution acting on the retaining structure (see e.g. Galli & di Prisco, 2013), and it cannot be disregarded by the designer when looking for the most accurate, safe and cost-effective solution. Traditional capacity-based design approaches do not explicitly take into account such complexity and they cannot completely fulfil the requirements of

*Corresponding author. Email: andrea.galli@polimi.it

the current performance-based standards, in particular when the effectiveness of a stabilising structure has to be assessed in terms of reduction of soil displacement rate. On the other hand, computational approaches based on continuum mechanics (such as those implemented in very well-known finite element or finite difference commercial codes, where even complex 3D geometries or advanced soil constitutive relationships are present) are often largely time consuming and computationally demanding. They can of course be considered as a powerful verification tool, but they can hardly be considered a helpful tool for a cheap and fast design optimisation. The present paper aims at presenting a simplified displacement-based design approach followed for a real case study. The innovative contribution consists in the definition of a rational and physically based design methodology for reducing the slope displacement rate, despite the lack of extensive and rich site characterisation data (as it is rather common in real case studies for geotechnical applications) and without invoking advanced computational tools. Monitoring data of the slope have been interpreted within the framework of a viscoplastic constitutive approach, and a simplified soil-structure interaction model based on the well-known P - γ curves method (see Section 4.3) was implemented into a user defined worksheet, thus allowing meaningful and fast simulations to be run. A pile stabilising system for a railway track has been conceived with the explicit aim of immediately reducing the soil displacement rate of the slope below a threshold value. The long-term behaviour of the system is also evaluated at the end of the assumed lifetime of the structure (50 years), both in terms of residual displacement rate and structural internal actions. Thanks to the high computational efficiency of the numeric tool, several installation scenarios have been easily simulated, and the optimum one have been identified in terms of both structural and railway safety.

2. Site characterisation and preliminary monitoring

The ballasted railway track under consideration is about 360 m long, and it is a part of a steep slope whose average inclination is close to 40° (Figure 1(a)). In the last decades, diffuse slow soil movements were observed (Figure 1(b)), and provisional intervention measures have already been realised by inserting steel rails vertically into the soil (Figure 1(c)).

2.1. Geotechnical characterisation

Three slope sections (labelled as S100, S300 and S500) have been considered as the most representative ones along the railway, and the design of the intervention measures has been optimised for those sections. In Figure 2(a), the topographic profiles of the three sections are reported (relative elevations Z are referred to the absolute elevation of section S100). In the following, due to the homogeneity of the slope and of the similarity of the profiles, only the details of section S500 are described, corresponding with the one where largest soil displacements have been observed. The geotechnical characterisation of the slope has been obtained by means of:

- (1) SCPT profile with a DPSH hammer (weight 73 kg, height 75 cm, cone angle 60° , diameter 51 mm),
- (2) continuous soil coring, up to a depth of 12.30 m below the ground level (whose position is also plotted in Figure 2(a)),

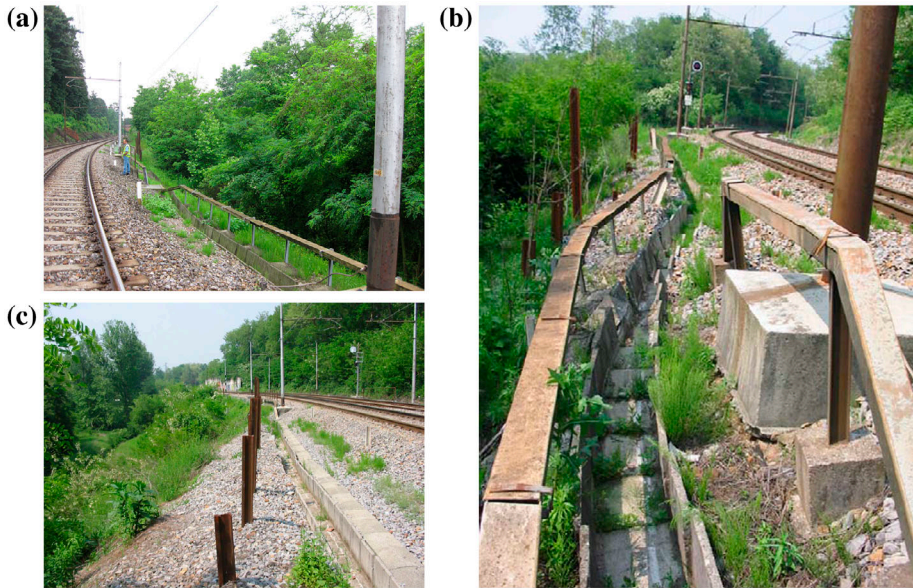


Figure 1. (a) View of the railway track; (b) lateral settlement of the soil; (c) provisional retaining system.

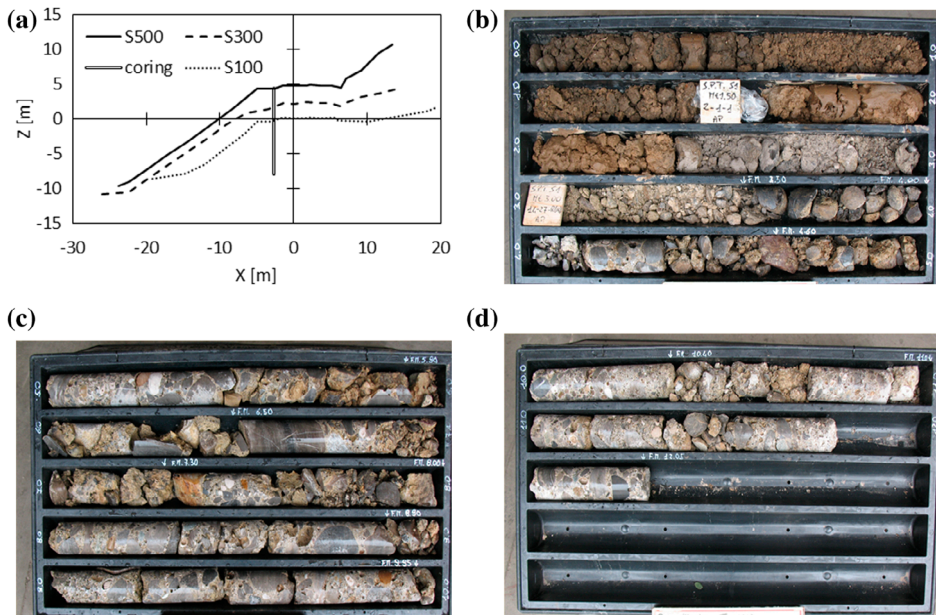


Figure 2. (a) Profiles of the three sections and trace of the coring in section S500. Continuous soil sampling at section S500: (b) 0–5 m; (c) 5–10 m; (d) 10–12 m.

- (3) laboratory analyses on two disturbed samples (labelled as *R1* and *R2* and taken at a depth of 1.5 and 3 m, respectively).

The visual inspection of the cored material (Figure 2(b)–(d)), allowed to recognise three different soil types:

- type *R*: a superficial layer of uncemented granular material, with an important fraction of fines, between 0 and 4 m approximately;
- type *D*: a layer of coarse granular material, sometimes weakly cemented, between 4 and 5.40 m;
- subgrade: a cemented material that can be assimilated to a weak rock of the “Ceppo Lombardo” type, up to the explored depth.

The interpretation of the SCPT penetrometer test (Figure 3(a)) gave the estimation of the soil friction angle (Figure 3(b)) and of a representative value of the Young modulus. It confirmed the presence of a superficial layer between a depth of 1 and 4 m, characterised by uniform value of the friction angle, and a second layer down to 5.40 m with increasing value of friction angle. Below this point, a blow number larger than 50 was obtained and the test was stopped. In Figure 3(b), dashed line and empty markers represent values judged to be not consistent with the actual soil type observed in the coring. The grain size distribution of the two samples *R1* and *R2* are plotted in Figure 4, whilst their characteristic grain size and Atterberg limits are listed in Table 1. Both of the samples present a high uniformity coefficient, and an important fraction of fines (diameter lower than .075 mm); sample *R2* in particular has a dominant fraction of fines (about 60%). No further mechanical characterisation by means of either standard or advanced laboratory tests (e.g. direct or simple shear tests, triaxial compression tests, resonant column tests ...) was possible, since undisturbed samples could not be bored in such kind of granular material. On the other hand, advanced sampling techniques (e.g. soil freezing) preventing any disturbance to the sample would have required a much more invasive and expensive intervention, which would have not been justified within the limited budget of the project.

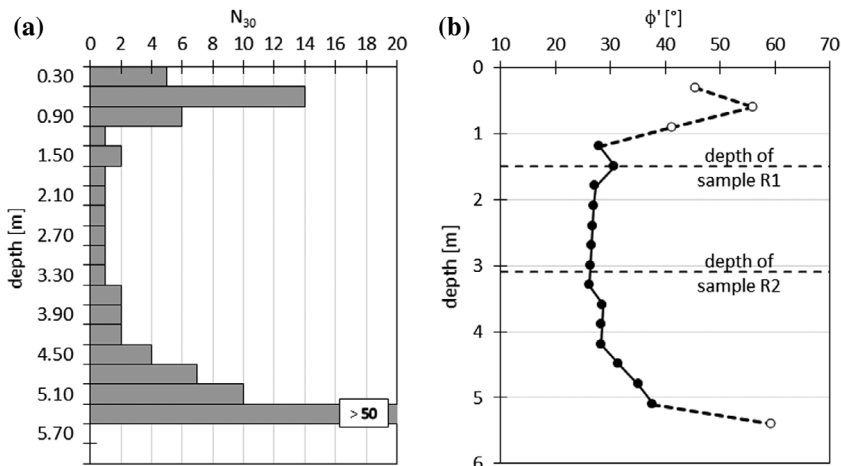


Figure 3. (a) SCPT-DPSH profile; (b) estimated values of the soil friction angle.

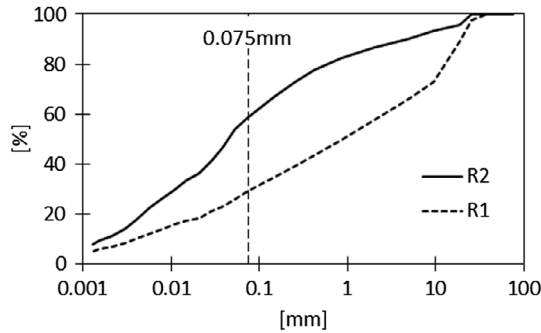


Figure 4. Grain size distribution of the two samples.

Table 1. Characteristic grain size and Atterberg limits of the two samples.

	R1	R2
Depth [m]	1.5	3
D_{10} [mm]	.004	.002
D_{50} [mm]	.884	.045
D_{60} [mm]	2.740	.085
Liquid limit	33%	32%
Plastic limit	23%	23%

2.2. Preliminary monitoring

A monitoring system, consisting in one inclinometer tube and one piezometer for each one of the representative sections of the slope, was installed along the railway track. The length (12 m for both the inclinometer and the piezometer) was chosen in order to reach a stable zone at the same depth of the base of the slope (Figure 2(a)). The first “zero” reading was taken on 23 October 2009 (Figure 5(a)) and the monitoring period lasted until 1 April 2011, corresponding to approximately 17.5 months. The soil displacement profiles recorded by periodic manual readings in proximity of section S500 are shown in Figure 5(b). No localisations of the soil displacement profile are recognised, but, on the contrary, a “diffuse” soil displacement pattern is rather evident in the slope. This observation allows inferring that:

- no actual failure mechanism has been activated yet into the slope;
- a stable but continuous accumulation of displacements has been observed and, thanks to the high ductility of the material, the same trend will be in principle expected in the next future;
- despite the presence of a weak rock as the Ceppo Lombardo, residual slope displacements are observed for a depth larger than 5.40 m.

This last consideration, in particular, suggests the possibility that the Ceppo is relatively highly fractured, and its behaviour is actually more similar to that of the upper layer of D type granular material. Temperature and daily rainfall values recorded by a public weather station near the site are plotted in Figure 5(c) and (d), respectively. Temperature record shows a seasonal excursion between -5 and $+30$ °C. Rainfall data do not show

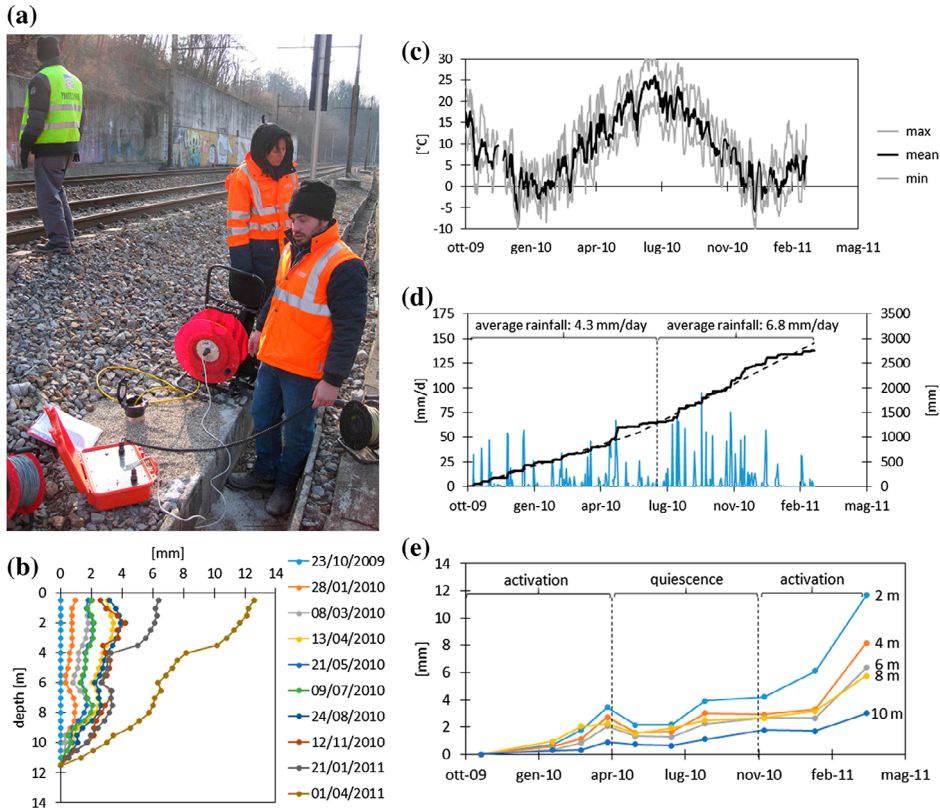


Figure 5. (a) Reading of the inclinometer; (b) evolution of soil displacement profile along depth; (c–d) temperature and rainfall data at the site; (e) displacement histories at five different depths.

any significant seasonal variation, but they are characterised by a quite uniform daily average rainfall of about 4.28 mm/day until June 2010. After that date, a bit higher daily average value of 6.82 mm/day is observed. Despite the remarkable cumulated rainfall height, the manual periodical piezometric readings didn't show any significant presence of water table into the slope (and they are not reported here for the sake of brevity), thus proving that, even in case of heavy rainfall events, groundwater is drained in a rather short time. The slope, from a hydraulic point of view, can then be considered partially saturated for the most part of the year.

Finally, the histories of displacement extracted from the inclinometer records at five different depths (2, 4, 6, 8 and 10 m) below the track level are reported in Figure 5(e). They clearly show different activation and quiescence phases, corresponding with the autumn–winter period and with the summer, respectively.

3. Slope stability analyses

Some preliminary slope stability analyses were performed by adopting the well-known Janbu limit equilibrium method of slices (Janbu, 1954). The site was modelled as a layered slope composed of three main materials: a superficial layer of type R, an intermediate layer of type D and a subgrade layer of Ceppo. According with inclinometer data

(Figure 5(b)), that demonstrated non-negligible soil displacement even at a relatively large depth without any sharp discontinuity, the Ceppo cannot be considered as a rigid bedrock. For the sake of safety, it was then characterised by using the same mechanical properties of material D, as commented in the previous paragraph. Consequently, rather than considering simple sliding mechanisms of layers *R* and *D* along the interface with the Ceppo, more general circular failure surfaces were assumed, allowing them even to intersect the underlying Ceppo layer. The presence of the railway embankment was modelled by introducing an additional zone of granular material reproducing the ballast (Figure 6(a)). The mechanical properties of the material *R* and *D* are listed in Table 2 as derived from the SCPT test interpretation, whilst the properties of the ballast were arbitrarily chosen in order to reproduce a cohesionless material with a relatively high friction angle ($\gamma = 18 \text{ kN/m}^3$, $\phi' = 40^\circ$). Due to the dominant presence of fines in the slope, a representative value of the undrained shear strength C_U for the entire slope was estimated as

$$\frac{C_U}{\sigma'_v} = 0.22 \cdot \text{OCR}^m, \quad (1)$$

inspired by the works of Skempton (1954, 1957) and Vardanega and Bolton (2011), with parameter $m = .8$. Because of the repeated loads given by train transit, the material can be considered as slightly overconsolidated (a value $\text{OCR} = 1.5$ has been considered); as a consequence, at a depth of about 4 m (corresponding with $\sigma'_v = 72 \text{ kPa}$) the expected value of the undrained strength computed by means of Equation (1) is approximately 23 kPa (Table 2). According with the monitoring data derived from the piezometers, no water table was introduced in the model; nevertheless, owing to the relatively high frequency of rainfall events, for the most part of the year the slope can be considered in a condition of partial saturation. From a mechanical point of view, this induces an apparent strengthening effect, that was modelled by assigning a small value of the cohesion to materials *R* and *D*. The chosen value (3 kPa) represents a lower boundary value for partially saturated materials (Baker & Frydman, 2009), and it was assigned with the aim of modelling in a simplified way even the strengthening effect offered at shallow depths by the vegetation. From a computational point of view, this choice will even prevent the formation of unrealistic very shallow sliding mechanisms. The presence of the trains was simply modelled as equivalent static loads $V_1 = V_2 = 100$ and $H_1 = H_2 = 5 \text{ kN/m}$, acting in vertical and horizontal direction, respectively, according to the guidelines of Reti Ferroviarie Italiane (1995).

The above-mentioned assumptions (in particular the last one referring to the modelling of the trainload) represent of course a set of very heavy simplifying hypotheses. The cyclic saturation–desaturation of the soil due to repeated rainfall events and the consequent infiltration process would in fact induce a complex hysteretic evolution of soil strength parameters in partially saturated condition. The train transit, moreover, results in an important dynamic load on the slope, inducing complex dynamic soil–ballast–railway interaction and 3D consolidation process to take place. All these phenomena are however characterised by a much higher frequency with respect to the frequency of manual inclinometer readings, and their effects cannot then be directly quantified by the monitoring data. The spirit of the paper, moreover, is not to present the most accurate academic exercise of numerical modelling, based on the most advanced numerical tools (which would never be of practical interest and applicability for the field engineer), but to build a simple and useful design approach, always leading

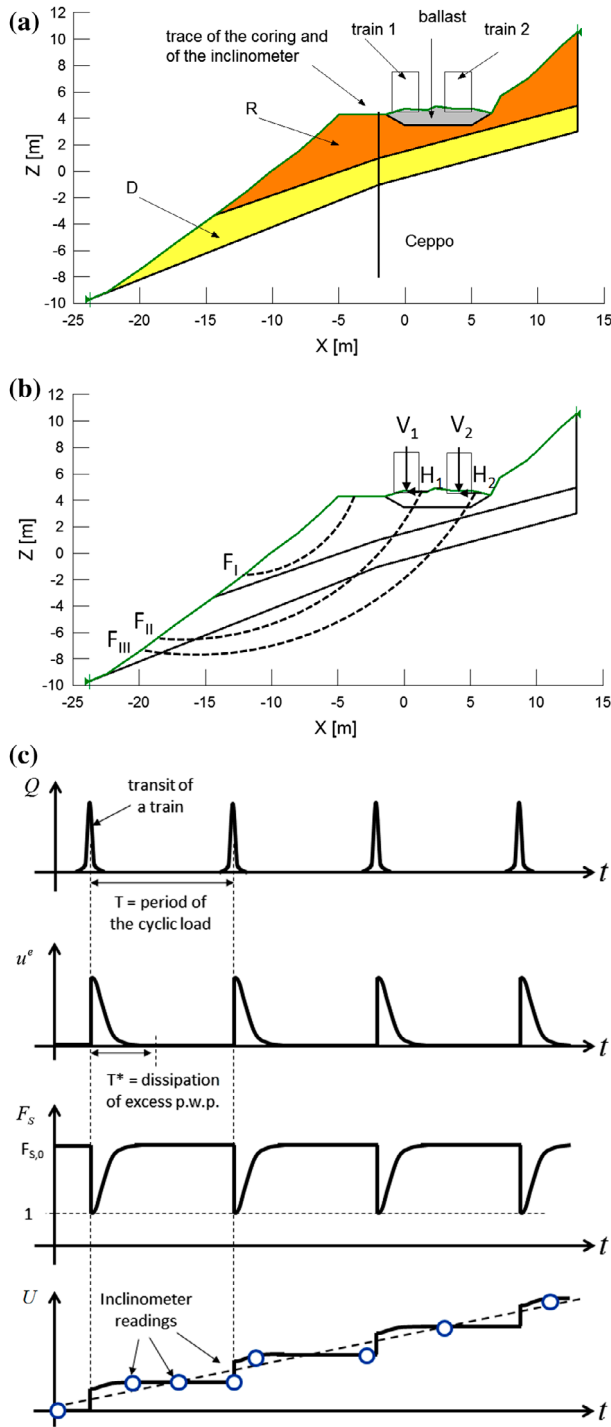


Figure 6. (a) Geotechnical model of the slope (section S500); (b) representative failure mechanisms in the slope; (c) phenomenological description of the displacement accumulation in the slope due to the repeated dynamic loads associated to the train transit.

Table 2. Geotechnical characterisation of the materials.

	R	D
Saturated unit weight [kN/m ³]	19	19
Friction angle [°]	28	35
Cohesion [kPa]	3	3
Undrained shear strength [kPa]	23	–
Young modulus [MPa]	5	10

Table 3. Results of the limit equilibrium slope stability analyses.

	F_I	F_{II}	F_{III}
Drained analysis, without external loads	1.15	1.28	1.66
Drained analysis, in presence of the trains	1.15	1.18	1.47
Undrained analysis, in presence of the trains	1.19	1.01	1.20

to a safe result. In this perspective, the above-mentioned assumptions allow to derive a simplified and reality-consistent framework, without the need for the final designer of invoking advanced and non-conventional computational tools.

Three different conditions were considered in the analyses to be representative:

- drained analysis, without external loads (i.e. the trains),
- drained analysis, in presence of external loads,
- undrained analysis, in presence of external loads.

For each case, three families of failure mechanisms were identified, as it is sketched in Figure 6(b):

- type F_I : failure of the slope not directly involving the railway tracks,
- type F_{II} : failure of the slope involving only one of the tracks,
- type F_{III} : failure of the slope involving both the railway tracks.

The results of the analyses are summarised in Table 3 in terms of global safety factors. Mechanisms of type F_I are the most critical, due to the high steepness of the slope, but they are not affected by the presence of the trains. Mechanisms of types F_{II} and F_{III} are on the contrary largely affected by the external loads, and their factor of safety is significantly reduced when introducing the loads given by the trains. Nevertheless, the application of loads in drained conditions does not induce the activation of a failure mechanism, since all the values of the factors of safety are significantly larger than one. As a consequence, these mechanisms would hardly be triggered by the train transit, which is a significantly less critical condition with respect to the assumed static loading scheme, and, on the basis of such limit equilibrium analyses only, no retaining structure at all would be judged to be necessary.

By considering the rapidity of the train transit, however, it would be more appropriate to assume an undrained analysis when modelling their effects on the slope. This assumption completely changes the results: all the mechanisms reduce their factor of safety and, in particular, mechanisms of type F_{II} reach a “quasi” failure condition, with a factor of safety very close to one. Due to the inertia of the soil mass, however, a fully localised failure mechanism cannot be activated in the short period corresponding with

the transit of one train, and the slope slowly dissipate the excess pore water pressure, coming back to a stable drained condition, in absence of external loads.

The repeated transit of the trains can hence be assimilated to an impulsive loading perturbation of amplitude Q and period T (Figure 6(c)), inducing at each cycle the generation of an excess pore water pressure u_e , with an immediate reduction of the safety factor F_S . The dissipation of the pressure u_e over the consolidation time interval T^* corresponds with the progressive increase in the global safety factor back to the initial (static) value F_{S0} computed in drained conditions without the presence of the train. This continuous variation between unloaded drained (stable) and loaded undrained (“quasi” failed) conditions, however, although not triggering a localised failure mechanism, induces the accumulation of small irrecoverable soil settlements U at each cycle. The time evolution of the total slope settlement is then represented by a complex function, with sudden activation and delayed slowdown phases; its precise description is however beyond both the purposes of this work and the practical interest of the field engineer. Moreover, the manual readings of the inclinometer data give only a time discrete estimation of this function, linearly increasing with time (as a first approximation) if the period T of the perturbations remains constant, i.e. if the frequency of the trains (and any other possible seasonal environmental condition) does not change. Such phenomenological explanation can be interpreted at the global macroscale of the entire slope as a “macro” creep problem, with progressive accumulation of permanent soil displacement at constant average value of the loads, and governed by a global viscosity parameter summarising all the time-dependent effects. This interpretation can in principle be extended to all the mechanisms of type F_{II} , independently of their radius, thus justifying the accumulation of a continuous soil displacements profile along the depth without any sharp discontinuity (as observed in Figure 5(a)).

4. Viscoplastic displacement-based design approach

The limit equilibrium analyses presented in the previous paragraph clearly proved that the intervention measure must be designed with the primarily aim to reduce the soil displacement rate, rather than to prevent the sudden activation of a global failure mechanism. Consequently, for this case study, it doesn't make sense to apply traditional force-based design approaches referred to Ultimate Limit State conditions and looking for a prescribed increase of the global safety of the slope, as it is usually done in slope stability analyses. A correct design methodology should rather refer to displacement-based design approaches, with respect to Serviceability Limit States. Limit equilibrium methods, based on rigid-perfectly plastic constitutive rules, obviously do not allow the designer to estimate the displacement of the system, i.e. to quantify the performance of this intervention measure on rational and objective criteria, neither immediately after the installation, nor along the whole life of the structure. This issue is even more important in presence of the railway track that requires very severe limitations on the allowable displacements in order to maintain the correct serviceability conditions. The simplest way to cope with such needs is to study the whole motion equation of the unstable soil mass, as suggested in Galli and di Prisco (2013), by adopting a rigid-viscoplastic constitutive framework.

4.1. Conceptual framework

In order to reproduce a continuous soil displacement profile as the one of Figure 5(b), the slope can be modelled as an infinite number of F_{II} type failure surfaces with the

same centre C and variable radius r , rotating of an angle ω around point C . For a generic failure surface, the viscoplastic motion equation then can be written (disregarding the soil mass inertia, since very slow soil displacement rates are here considered) by imposing the equilibrium of moments:

$$M_i(r) - M_r(r) = \eta \cdot \dot{\omega} \cdot r^2 \quad (2)$$

where $M_i(r)$ represents the driving action due to the self-weight W of the soil mass and of the external loads, $M_r(r)$ represents the limit shear resistance along the failure surface and the term on the right-hand side represents the viscous resistance there mobilised, proportional to the angular velocity of the soil mass. In Equation (2), only positive values of the angular velocity will of course be considered. This latter term is governed by a “global” viscosity parameter η summarising all the time-dependent effects, including train transit, seasonal climate changes and soil moisture variations. Following the phenomenological interpretation proposed in Section 3, parameter η can be calibrated by interpolating the preliminary inclinometer data, and solving Equation (2) before the installation of the retaining structure for any admissible radius r (Figure 7(a)), thus reproducing the observed soil displacement profile. The obtained value of η can be considered representative of the system, unless significant changes in the frequency of the train transit or of seasonal weather conditions take place.

Two main simplifying hypotheses have then been introduced:

- (i) the value of parameter η does not change in presence of the structure and
- (ii) the soil displacement rate after the installation of the structure is constant.

Under the first hypothesis, Equation (2) can be solved again by introducing the stabilising action A given by the retaining structure (Figure 7(b)), and computing the new soil displacement rate. The term A is in general split into an active component A_0 (due e.g. to a pretensioning action) independent of the soil displacement field, and in a passive component A_p depending on the relative displacement between the soil and the structure. Consequently, the action A can only be evaluated by solving at each time step a soil-structure interaction problem, in order to explicitly compute the time evolution of the system. For the sake of simplicity, however, it will be assumed in the following that the dominant component of A is the pretensioning action A_0 , inducing an important immediate reduction of the soil displacement rate of the slope. As an engineering approximation and according to hypothesis (ii), this new soil displacement rate will be considered constant after the installation of the structure, and the long-term expected amplitude of the soil displacement profile will then be computed accordingly. The effectiveness of the retaining structure can then be evaluated directly on this quantity, thus giving a rational and objective criterion for the estimation of the performance of the stabilising system directly based on the main parameter of interest for the slope, i.e. its displacement amplitude. Finally, once the long-term soil displacement profile is known, the corresponding displacements of the structure and its internal state of stress can be evaluated, in order to check both SLS and ULS conditions.

As a brief comment of the two main hypotheses (i) and (ii), it is worth noting that the presence of the structure will certainly modify the global viscous parameter η of the system, and a precise forecast of this effect is almost impossible. The retaining structure will in fact induce significant local modifications to the soil displacement field close to piles (the so-called “near field”) with respect to the initial condition of unreinforced

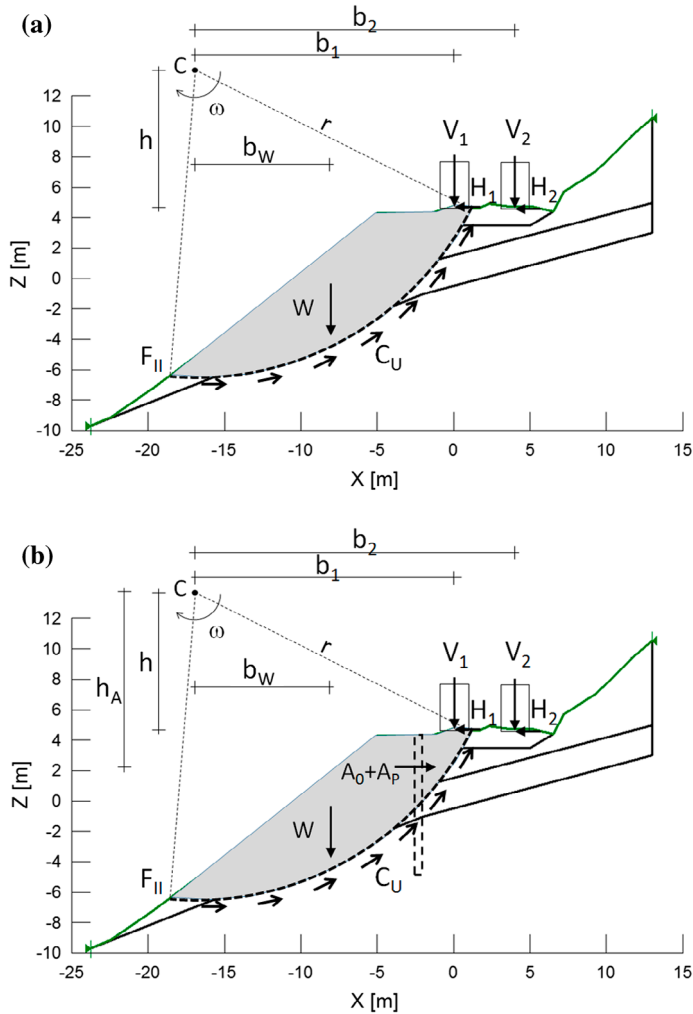


Figure 7. Equilibrium of the soil mass (a) without the retaining structure and (b) in presence of the retaining structure.

slope. Important 3D effects will be then mobilised, finally resulting in an increase in parameter η . Moreover, thanks to the high ductility of the materials constituting the slope, the term A_P tends to increase with increasing soil displacement amplitude, and the actual soil displacement rate is progressively reduced during the whole lifetime of the structure. Hypotheses (i) and (ii) are then both conservative, since they lead in principle to an overestimation of the long-term soil displacement.

Finally, from a mechanical point of view, the conceptual framework briefly outlined here above combines together two different characteristic times. The visco-plastic stability analysis of the slope, in fact, is run under the assumption of an undrained mechanical response of the system (i.e. short term), since the cyclic loads given by the train transit can be considered rapid with respect to the characteristic consolidation time T^* of the slope. The soil-structure interaction force A , on the contrary, is evaluated by means

of an effective stress analysis (i.e. long term, see Section 4.3), since it depends on the permanent soil displacements accumulated into the slope.

4.2. Calibration of global viscosity parameter η

The calibration of parameter η was obtained by considering the data derived from the inclinometer records during the first year of monitoring activity (23 October 2009–12 November 2010), corresponding with one complete cycle of activation and quiescence phases (Figure 5(e)). The terms on the left-hand side of Equation (2) have been explicitly computed as

$$M_i(r) = W(r) \cdot b_w(r) + V_1 \cdot b_1 + V_2 \cdot b_2 + (H_1 + H_2) \cdot h \quad (3)$$

whilst

$$M_r(r) = \int_{F_{II}} C_U \cdot r^2 \cdot d\omega \quad (4)$$

where C_U is in general variable along the failure surface depending on the depth below the ground level according to Equation (1). A value of the undrained strength linearly increasing from zero to approximately 90 kPa at a depth of 15 m has then been considered, consistently with the value of C_U listed in Table 3. The back analysis on the monitoring data allowed to estimate a value of the global viscosity parameter η . Although a different value of η should in principle be calibrated for each value of the radius r (thus allowing to exactly reproduce the displacement rate profile), for the sake of simplicity a constant average value of $\eta = 8 \times 10^{11}$ kPa s was estimated independently of r , since the obtained displacement rate profile satisfactorily reproduces the monitored data (Figure 8).

4.3. Modelling the soil–pile interaction

For the specific problem under consideration (Figure 9(a)) piles are installed vertically, and, except for their own weight, the dominant component of the active loads is the horizontal one. For the sake of simplicity, it has then been assumed that both the ground anchors and the soil displacement direction lie in the horizontal plane, i.e. normally to pile axis. Several works in Literature describe the behaviour of piles subject to lateral loads (Broms, 1964; Fan & Long, 2005; Georgiadis & Butterfield, 1982; Ito & Matsui, 1975; Matlock & Reese, 1960; Reese, Cox, & Koch, 1974; Reese, Isenhower, & Wang, 2006; Reese & Welch, 1975; Viggiani, 1981), especially by employing a simplified approach based on P – y curves. These latter describe the interaction force on each single slice of the pile as a function of its lateral deflection, i.e. the difference between the horizontal pile displacement, u , and that of the surrounding soil, U . The pile is then discretised as an array of beam finite elements connected to the soil by means of uncoupled springs (Figure 9(b)), and a known soil displacement profile is imposed at the base of the springs (corresponding with the “far field” soil displacement profile). Among several possible approaches modelling the P – y curves at different depths as complex non-linear functions (Figure 9(c)), in the following a simplified elastic perfectly plastic model has been employed. In particular, the horizontal stiffness k_H of the springs have been calibrated by assimilating each slice of the pile to a buried shallow foundation, subject to horizontal load (Gazetas, 1991)

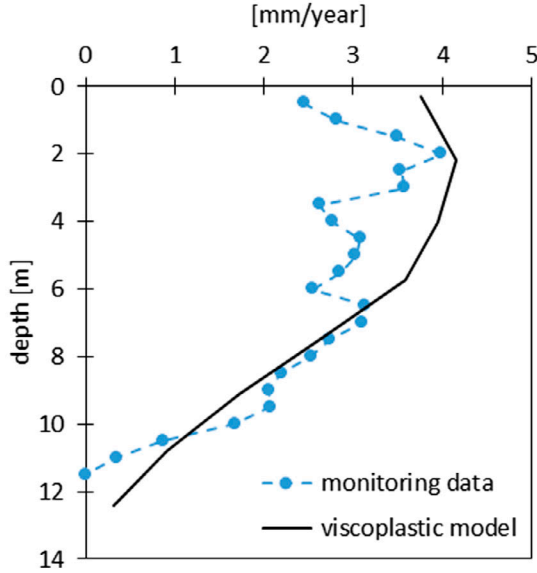


Figure 8. Comparison between the soil displacement rate derived from monitoring data and from the calibration of the viscoplastic model for the slope.

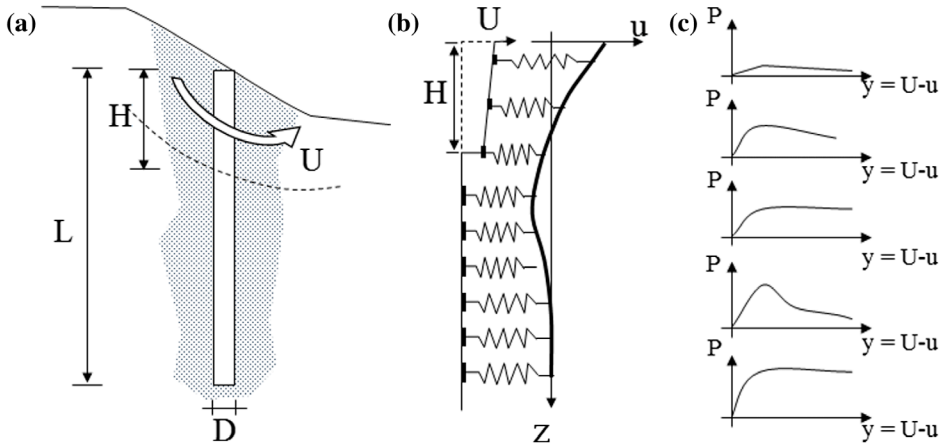


Figure 9. (a) Schematic view of a stabilising pile interacting with an unstable soil mass; (b) modelling the soil–pile interaction by means of uncoupled non-linear springs; (c) example of non-linear P - y curves.

$$k_h = \frac{4G}{2-\nu} \left(1 + 0.15 \sqrt{\frac{z}{D} + \frac{1}{2}} \right) \quad (5)$$

where G and ν are the elastic shear modulus and the Poisson coefficient estimated for the soil, respectively; z and D are the depth of the considered slice of the pile below ground surface and the pile diameter. The interaction between piles has been accounted

in a simplified manner: the limit value of the horizontal loads (corresponding with the yielding of the non-linear soil–pile interaction springs) is evaluated as a weighted average between the limit load of an isolated pile and the limit load of a continuous bulkhead. The first one is computed according with the procedure proposed by Audibert and Nyman (1977)

$$\frac{H_{L,pile}}{D \cdot L_s} = \gamma \cdot z \cdot N_q(z/D, \phi') \quad (6)$$

where γ is the unit weight of the soil, L_s is the length of the slice and N_q is a horizontal bearing capacity factor (Figure 10(a)), depending on the soil friction angle ϕ' and on the relative depth z/D of the considered slice. The second one is

$$\frac{H_{L,bulkhead}}{D \cdot L_s} = \gamma \cdot z \cdot (K_P - K_A) + 2c' \cdot (\sqrt{K_P} - \sqrt{K_A}) \quad (7)$$

where c' is the cohesion of the soil, and K_P and K_A are its passive and active earth pressure coefficients. As a consequence, the horizontal limit load of each non-linear spring is computed as

$$H_L = \alpha \cdot H_{L,bulkhead} + (1 - \alpha) \cdot H_{L,pile} \quad (8)$$

The weight α depends on the ratio between the pile spacing, S , and its diameter D . A simple linear decreasing trend from one to zero has been assumed, for S/D values ranging between 1 and 4 (Figure 10(b)), inspired to the efficiency coefficient for pile groups proposed by Reese and Van Impe (2001). The choice of the optimum spacing can then be obtained by maximising the values of H_L with respect to S .

By imposing the equilibrium between the loads acting on the pile and the soil reactions given by the P – y curves, it is possible to compute the deformed shape of the pile and its internal state of stress for a given soil displacement profile. Given the non-linearity of the problem, an explicit finite difference numerical solution has been implemented in a Matlab code, and the problem was step-wise solved by employing at each step a tangential stiffness matrix of the system, obtained by combining the pile stiffness matrix (assumed to be elastic, for the sake of simplicity) with a global soil stiffness matrix. In this framework, the presence of the ground anchor can be modelled as an additional spring, whose mechanical behaviour is assumed to be linear and elastic. Further details can be found in Galli, Cocchetti, and di Prisco (2011), and Galli and di Prisco (2013).

5. Structural design

The chosen slope stabilising system consists in fibre reinforced concrete (FRC) piles connected to each other at the top by means of a FRC precast beam, in which pre-stressed ground anchors will be installed (Figure 11(a)). This type of structure allows to significantly reduce the cost and time of the intervention with respect to traditional retaining systems (e.g. continuous cast in place walls, or deep bulkhead), to actively sustain the slope (thus immediately reducing the soil displacement rate), to control the railway displacement during the installation phases, to actively support even deep soil layers (thus reducing the required length of the piles). The structural design optimisation has been iteratively achieved by:

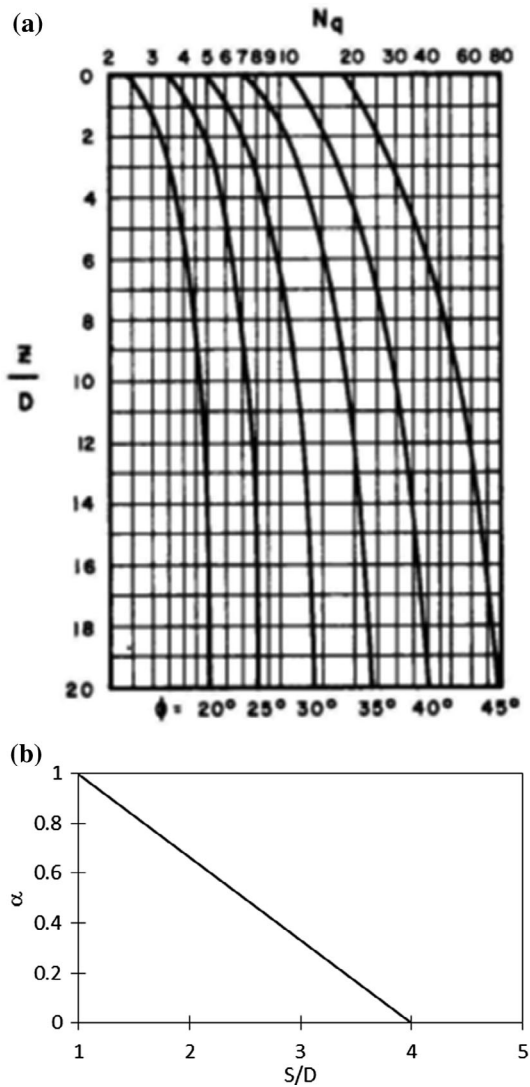


Figure 10. (a) horizontal bearing capacity factor (after Audibert & Nyman, 1977); (b) definition of the weight function α .

- (i) choosing a pile typology,
- (ii) choosing the geometry of the intervention (position and spacing of piles),
- (iii) choosing the active tensile force (pre-stressing) on the ground anchor,
- (iv) evaluating the immediate soil structure interaction forces (term A_0),
- (v) checking the pile and anchor safety,
- (vi) evaluating new soil displacement rate profile,
- (vii) evaluating the expected long-term soil displacement, i.e. at the end of the life-time of the structure,
- (viii) computing the corresponding long-term pile–soil interaction forces (A_p),
- (ix) evaluating the long-term tensile action in the ground anchor,

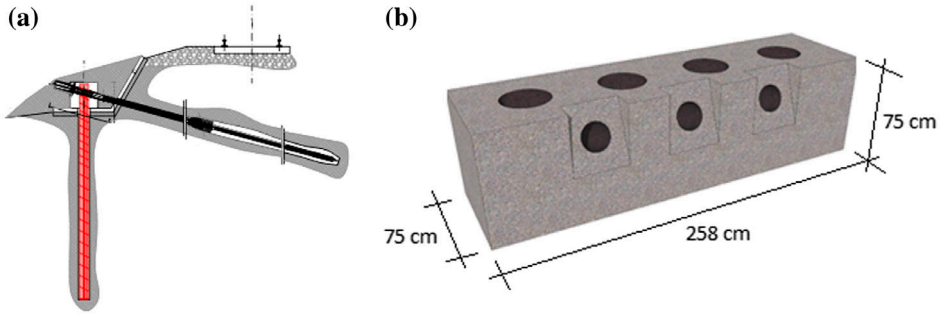


Figure 11. (a) Schematic view of the slope stabilising piles reinforced with a pre-stressed ground anchor; (b) precast FRC beam.

- (x) checking the long-term pile safety,
- (xi) evaluating the residual long-term expected soil displacement rate profile.

The steps (i)–(ix) have been repeated until all the checks were satisfied and the residual soil displacement rate has been considered sufficiently low. During the design phase, a hierarchy of the resistance was defined with the aim of increasing the robustness of the structure. For this motivation, the expected sequence of failure modes is (1) anchorage slipping, (2) flexural failure of pile and (3) shear failure of the pile.

5.1. Description of the structure

The structure has been conceived as a modular retaining intervention measure, composed by 78 precast FRC beams whose dimensions are $.75 \times .70 \times 2.58$ m. The total length of the intervention is 366 m. Each beam connects four drilled and cast in place piles (Figure 11(b)) and it is even designed in order to host up to three sub horizontal anchors, although only one permanent anchor per beam will be installed (the installation procedure will follow the prescriptions of the standard EN 1537-2002). Each anchor is composed of .6" harmonic steel strands (EN 10138), and it will have a total length of about 21 m, including 12 m of deep anchoring bulb.

The piles will have an external diameter D of 300 mm and a total length L of 5.75 m (including the part within the FRC beam). They will be installed with a spacing S of 600 mm (a spacing to diameter ratio lower than 4 is generally recommended to ensure the formation of a relevant arching effect; see e.g. Kourkoulis, Gelagoti, Anastopoulos, & Gazetas, 2011). Fibre Reinforced Concrete, together with conventional longitudinal steel reinforcement rods have been employed to guarantee a quasi-ductile behaviour of the pile section in terms of bending response (in Figure 12 the expected mechanical response computed according to the Model Code 2010 is shown; a limit value for the pile bending moment of 150 kNm has been assumed). The main contribution of fibre addition will be the increase of shear strength, the control of crack opening and an important contribution against fatigue loads. The dimensions of the pile and the mechanical properties of the materials have been optimised by following the aforementioned steps (i)–(ix).

Particular attention has been devoted to develop an innovative installation technique, capable of limiting the settlement of the railway during the excavation and cast in place

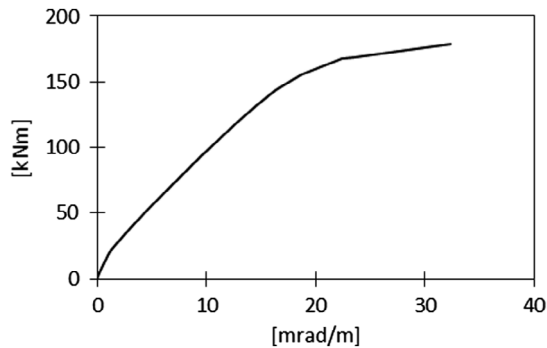


Figure 12. Moment-curvature behaviour of pile section in pure bending according.

phases; the particular choice of precast elements allows even to speed up the installation phases, without the need of stopping the regular daily transit of the trains. A detailed description of the installation technique, as well as further details on structural design are beyond the scope of the present paper, and they have already been discussed in Galli, Bassani, di Prisco, and di Prisco (2014).

6. Immediate and long-term expected response of the system

The goal of the intervention is to reduce the horizontal soil displacement rate below a limit of .5 mm/year, value that can be considered negligible for management purposes. Pre-stressing of the ground anchors, however, could induce even significant immediate uplift of the railway track; in order to prevent such risk, a combined active-passive strategy for the structural behaviour has been adopted. The assigned value of the pre-stressing tensile force (active behaviour) has been chosen in order to get an immediate significant reduction of the soil displacement rate, without inducing excessive uplift of the railway, or large values of pile bending moments. Then, owing to the residual soil displacements rate, the structure will behave as a passive retaining system during its life, by progressively increasing the soil-pile interaction loads and correspondingly reducing the residual soil displacement rate. The balance between the active and passive behaviour must be optimised depending on the expected performance of the intervention measure. Several installation scenarios have been simulated by considering four different levels of pre-stressing load in the ground anchors, corresponding to 25, 50, 75 and 100% of the maximum design load of 150 kN/m (expressed here per unit length of the intervention), chosen as a limit value to prevent cracking in the FRC beams and into the piles. For each scenario, the analyses of the system have been run according to the visco-plastic model previously described and the results have been plotted in Figure 13 in terms of

- (a) residual soil displacement rates (positive values represent downward velocities),
- (b) loads distribution and
- (c) bending moment on piles,
- (d) profile of pile displacements (positive values represent uphill displacements),

both for the immediate and long term response of the system, by assuming a target lifetime of 50 years. As expected, the increase in the prestressing value induces larger and

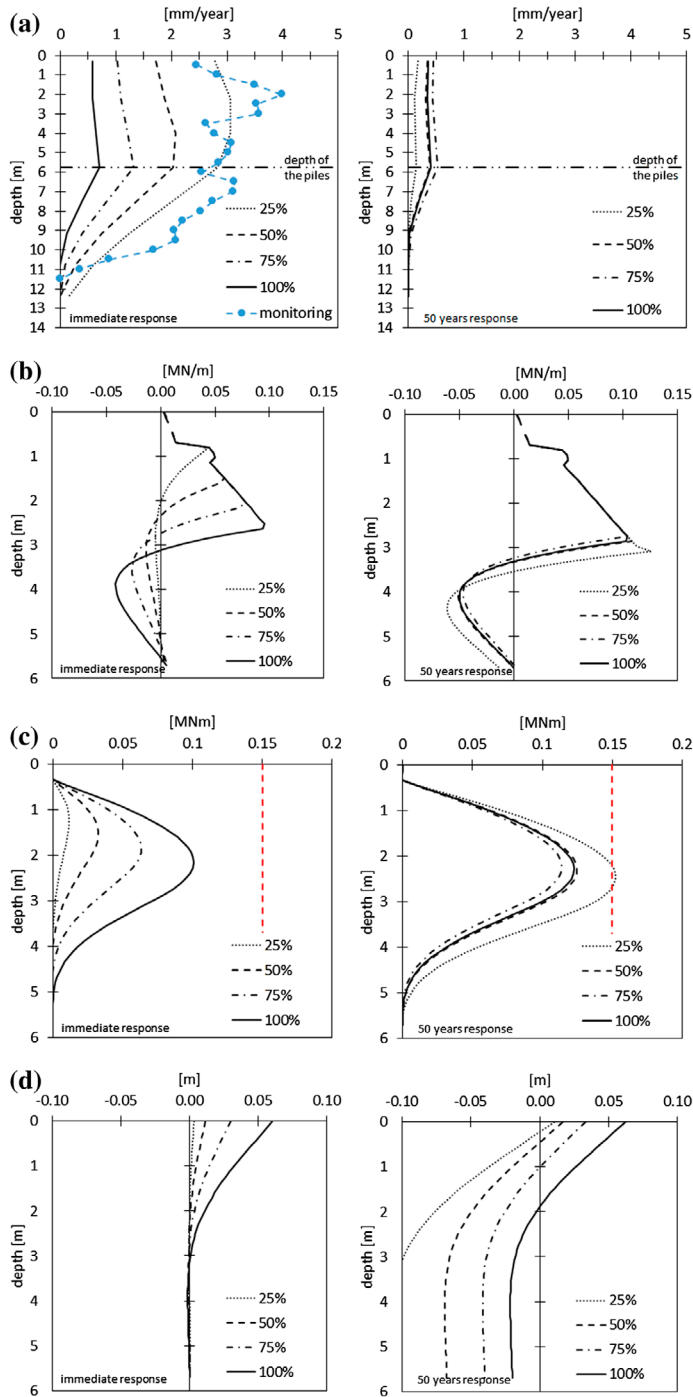


Figure 13. Comparison between immediate and long-term response of the system for different levels of the pretensioning force in the ground anchors: (a) soil displacement rates, (b) distribution of the horizontal loads acting on the pile, (c) pile bending moment and (d) pile displacements.

Table 4. Fifty years long-term response of the system for the different scenarios.

Prestressing value	25%	50%	75%	100%
Average soil displacement [mm]	104	67	40	20
Tensile force in anchors [kN/m]	193.3	171	161.6	169.2

larger immediate reduction of the soil displacement rate profile, but, as a consequence, increasing values of the pile bending moment (which, however, do not reach the limit value of 150 kNm for the pile section) and of the upward pile displacements (up to 6 cm). This latter point can be particularly detrimental for the serviceability of the railway, since a slight modification in the layout (especially in case of uplift of the rails) may induce significant reduction of the speed limit for the trains. The analysis of the immediate response of the system would then suggest adopting an installation scenario with a limited value of the prestressing force imposed to the anchors (i.e. 25% of the design value).

On the other hand, according to the long-term response (50 years), all the scenarios show acceptable final values of soil displacement rate (all the curves are below the required limit of .5 mm/year), with a minimum value corresponding with the scenario with an initial prestressing action equal to the 25% of the design load. According to the data listed in Table 4, however, this scenario corresponds with the maximum values of both the long-term average soil displacement (larger than 100 mm) and the tensile action in the ground anchors. Consequently, this scenario cannot be considered acceptable for the 50 years safety and effectiveness of the intervention measure.

By summarising all the considerations reported here above, among the four tested scenarios, the optimum one appears to be that corresponding with an initial prestressing load in the ground anchor equal to 75% of the design load. This scenario in fact

- (i) minimises the long-term tensile action in the ground anchors,
- (ii) does not allow excessive soil and pile displacements to develop (neither immediately after the installation, nor at the end of the lifetime of the structure), and
- (iii) does not induce long-term bending moments in the pile significantly larger than those induced by the other scenarios.

6.1. Additional remarks

As it was previously cited, the long-term results discussed here above could be significantly overestimated with respect to the real ones. The two main reasons depend on the two simplifying hypotheses introduced in Section 4.1. The global viscous parameter η is in fact kept constant after the installation and equal to that previously calibrated on the preliminary monitoring data, whilst the presence of the structure is actually expected to induce an increase of the global viscosity of the system. On the other hand, the soil displacement rates after the installation are considered constant during the whole lifetime of the structure, whilst they actually tend to reduce thanks to the passive behaviour of the system. The validity of the two cited assumptions will be verified only upon the interpretation of the monitoring data along a convenient time window after the installation, but they will ensure to get safe estimation of the long-term design control variables. Nevertheless, the presented approach is of general validity, and, owing to its high computational efficiency, the results can be easily improved. By back analysing the monitoring data for a significant time window (e.g. at least one year) after the

installation of the structure, in fact, a “new” value of the global viscosity parameter can be calibrated, thus empirically including the effect of the structure. Such considerations allow to stress even the importance of the monitoring system not only in the preliminary design phase, but even for optimising the long-term management of the structure, and for the verification of the design hypotheses.

Moreover, from a computational point of view, the long-term behaviour (i.e. 50 years, in the present case) can be studied by splitting the entire lifetime of the structure in several steps. By solving the viscoplastic problem and the soil–pile interaction problem for each step, it is possible to update the values of the soil–pile interaction forces and of the soil displacement rates at the end of each steps, thus refining the numerical results up the desired precision.

From a design point of view, finally, it is worth noting that the presented combined active-passive design approach, based on a viscoplastic description of the slope stability, allowed to optimise the length of the piles (about 5 m) with respect to the whole thickness of the soil moving mass (approximately 12 m see Figure 5(b)). At large depth, in fact, very small soil displacements are observed (Figure 5(b)) and, consequently, negligible values of the soil–pile interaction forces would be mobilised, with almost nil effect on the stabilisation of the slope. Despite the reduced length, the pile is efficient in reducing the soil displacement rate even for deep soil strata, as is evident in Figure 13(a), thus saving a large part of the cost of the intervention.

7. Conclusions

An innovative displacement-based procedure for the design of slope stabilising piles have been illustrated with reference to a real case study of a railway embankment on a steep slope. A key point is the correct interpretation of field monitoring data, allowing to define the actual soil displacement rate profile into the slope. A simplified viscoplastic analysis of the slope, combined with an ad hoc soil–pile interaction model, allowed to conveniently optimise the design of the intervention measure in terms of position, length and diameter of the piles, as well as in terms of the prestressing tensile load assigned to the ground anchors, without making use of complex 3D dynamic soil–structure numerical analyses.

The viscoplastic numerical scheme allowed even to foresee (although in a simplified way) the long-term behaviour of the structure, and thus to optimize the design and the installation procedure both with respect to immediate and long time performance of the intervention measure.

As it was highlighted into the text, the proposed results (especially in terms of long-term soil displacement) can be significantly overestimated. If, on one hand, they thus represent a safe side estimation of the long-term performance of the structure, on the other hand they can be remarkably improved during the lifetime of the structure by continuously updating the monitoring data and by running new viscoplastic analyses. This point also stresses the fundamental role of the monitoring system not only for the interpretation of the phenomenon and for the optimum design of the structure, but even for the long-term managing of the stabilising system and the definition of possible corrective strategies.

Acknowledgement

The authors want even to thank prof. Claudio di Prisco and prof. Marco di Prisco for their support in the research work.

Disclosure statement

No potential conflict of interest was reported by the authors.

Funding

This research was partially funded by the Italian Ministry of Education, University and Research (MIUR), within the PRIN project: “La mitigazione del rischio da frana mediante interventi sostenibili”.

ORCID

Andrea Galli  <http://orcid.org/0000-0002-4754-5206>

References

- Audibert, J. M. E., & Nyman, K. J. (1977). Soil restraint against horizontal motion of pipes. *Journal of Geotechnical Engineering Division, ASCE*, 103, 1119–1142.
- Baker, R., & Frydman, S. (2009). Unsaturated soil mechanics. *Engineering Geology*, 106, 26–39.
- Broms, B. B. (1964). Lateral resistance of piles in cohesive soils. *Journal of the Soil Mechanics and Foundations Division, American Society of Civil Engineers*, 90, 27–63.
- EN 10138. Prestressing steel. CEN, Brussels.
- EN 1537-2002. Special Geotechnical Works - Ground Anchors (in Italian). CEN, Brussel. http://www.tandf.co.uk/journals/authors/style/reference/tf_APA.pdf.
- Fan, C. C., & Long, J. H. (2005). Assessment of existing methods for predicting soil response of laterally loaded piles in sand. *Computers and Geotechnics*, 32, 274–289.
- Galli, A., Bassani, A., di Prisco, C., & di Prisco, M. (2014, November 6–8). *Design of slope stabilizing piles for a railway embankment (in Italian)* (pp. 435–444). XX Congresso CTE, Milano.
- Galli, A., Cocchetti, G., & di Prisco, C. (2011, September 11–15). A simplified numerical approach for studying the pile-landslide interaction in hard soils (pp. 1347–1352). Proceeding of 15th European Conference on Soil Mechanics and Geotechnical Engineering, Athens.
- Galli, A., & di Prisco, C. (2013). Displacement-based design procedure for slope-stabilizing piles. *Canadian Geotechnical Journal*, 50, 41–53.
- Gazetas, G. (1991). *Foundation vibrations. Foundations engineering handbook* (pp. 553–593). New York, NY: Chapman and Hall.
- Georgiadis, M., & Butterfield, R. (1982). Laterally loaded pile behaviour. *Journal of Geotechnical Engineering Division, American Society of Civil Engineers*, 108, 155–165.
- Ito, T., & Matsui, T. (1975). Methods to estimate lateral force acting on stabilizing piles. *Soils and Foundations*, 15, 43–59.
- Janbu, N. (1954). *Application of composite slip surface for stability analysis*. European Conference on Stability Analysis, Stockholm, Sweden.
- Kourkoulis, R., Gelagoti, F., Anastasopoulos, I., & Gazetas, G. (2011). Slope stabilizing piles and pile-groups: Parametric study and design insights. *Journal of Geotechnical and Geoenvironmental Engineering*, 137, 663–677.
- Matlock, H., & Reese, L. C. (1960). Generalized solution for laterally loaded piles. *Journal of the Soil Mechanics and Foundations Division, American Society of Civil Engineers*, 86, 63–91.
- Model Code 2010 – fib Model Code for Concrete Structures 2010.
- Reese, L. C., Cox, W. R., & Koch, F. D. (1974). *Analysis of laterally loaded piles in sand* (Vol. II, pp. 473–484). Proceedings Offshore Technology Conference, Houston, TX, Paper No. 2080.
- Reese, L. C., Isenhower, W. M., & Wang, S. T. (2006). *Analysis and design of shallow and deep foundations*. Hoboken, NJ: John Wiley.
- Reese, L. C., & Van Impe, W. F. (2001). *Single piles and pile groups under lateral loading*. Rotterdam: A.A. Balkema.
- Reese, L. C., & Welch, R. C. (1975). Lateral loading of deep foundations in stiff clay. *Journal of Geotechnical Engineering Division, American Society of Civil Engineers*, 101, 633–649.

- Reti Ferroviarie Italiane. (1995). Loads for railway bridges. Recommendation for design, construction and verification (in Italian), RFI I/SC/PS-OM/2298_1995.
- Skempton, A. W. (1954). Discussion: *Sensitivity of clays and the c/p ratio in normally consolidated clays*. *Proceedings of the American Society of Civil Engineers, Separate*, 478, 19–22.
- Skempton, A. W. (1957). Discussion: *Further data on the c/p ratio in normally consolidated clays*. *Proceedings of the Institution of Civil Engineers*, 7, 305–307.
- Vardanega, P. J., & Bolton, M. D. (2011). Strength mobilization in clays and silts. *Canadian Geotechnical Journal*, 48, 1485–1503.
- Viggiani, C. (1981). *Ultimate lateral load on piles used to stabilize landslides* (Vol. 3, pp. 555–560). *Proceedings of the 10th International Conference on Soil Mechanics and Foundation Engineering*, Balkema, Rotterdam, Netherlands.